Journal of Network Intelligence
Taiwan Ubiquitous Information
 ISSN 2414-8105
Volume **10**, Number **4**, November **2025**

Track and Field Training Behavior Monitoring Based on Conjugate Material Smart Sensors and Neural Networks

Meng Lu

Department of Physical Education
Anhui Sanlian University
Hefei 230601, P. R. China
95219701@qq.com

Yang Wang*

Department of General Education
Anhui Xinhua University
Hefei 230088, P. R. China
20470649@qq.com

Yun-Fei Zhu

Thailand Northwestern University
Chiang Mai 20260, Thailand
1468059575@qq.com

*Corresponding author: Yang Wang
Received July 4, 2024, revised December 18, 2024, accepted June 8, 2025.

Abstract. *Training behavior monitoring is one of the key technologies to realize the intelligent and refined management of track and field training sports, which can improve the training methods and enhance the sports level by monitoring the training behavior of athletes. In this article, for the issue of feature redundancy and neglect of key features in behavioral monitoring methods, which leads to low monitoring accuracy, a track and field training behavior monitoring method based on conjugate material intelligent sensors and neural networks is designed. Firstly, the training behavior data of track and field athletes are collected relied on Conjugate Intelligent Sensors (CIS), and the collected behavior data are denoised using wavelet analysis. Second, multivariate statistical analysis is used to study the internal relationship between multiple sensor signal variables to extract the features hidden in these potential variables, and in order to reduce the feature redundancy, principal component analysis is used for feature dimensionality reduction to highlight the effective dimensions. Finally, the attention mechanism is introduced into one-dimensional Convolutional Neural Network (CNN) to enhance the key behavioral features, and the LSTM layer is used to learn the temporal features among the behavioral features cyclically, and the weights are applied in the fully-connected layer to complete the classification and monitoring of the behaviors. The experimental outcome implies that the suggested method has high accuracy, precision, recall and F1-Score, which verifies the effectiveness of the designed method.*
Keywords: conjugate intelligent sensor; behavioral monitoring; wavelet analysis; principal component analysis; convolutional neural network

1. **Introduction.** As the science and technology growing, big data and artificial intelligence have been widely used in various fields. In the field of athletics, sports training is a crucial task [1]. Athletic training is the key link to improve the athletic level of athletes. Most of the muscle injuries that occur in track and field athletes during training are due to excessive training intensity and long training time, and accurate monitoring of sports training behavior is the key to improve the training effect [2, 3]. Track and field athletes are involved in a wide variety of unsafe behaviors during exercise, such as fatigue training, distraction training, etc. These behaviors are often not easy to be monitored manually. These behaviors are often not easy to be monitored and identified manually, so intelligent technological means are needed for monitoring and early warning [4, 5]. However, behavior detection of track and field athletes involves several issues, and how to classify the behaviors of track and field training and construct efficient behavior detection models are the difficulties and challenges that need to be addressed.

1.1. **Related work.** Chen et al. [6] used a respiratory sensor to capture and monitor training behavioral actions in track and field. Xue et al. [7] suggested a Support Vector Regression (SVR) model for accurate estimation of basic gait parameters extracted from instrumented insoles for walking and running. Balli et al. [8] integrated a light sensor and a microcontroller embedded in a device that can be worn as a sports watch to classify behaviors using random forests. Welch et al. [9] placed accelerometers on the wrists and waists of track and field athletes to perform coarse-grained classification to determine the type of behaviors. Xia et al. [10] captured gyroscope sensor signals to identify training behaviors of track and field athletes. With the rapid development of wearable devices, Lee et al. [11] proposed the application of conjugated materials to smart sensors, and the coupling of small bandgap and large bandgap conjugated semiconductors can effectively improve the efficiency of monitoring. Shanthini et al. [12] designed a set of track and field athletes' training behavior data acquisition device based on conjugated material accelerometer sensors, and utilized the K-means mean-value clustering algorithm to analyze the collected pre-training behaviors. clustering algorithm to classify the collected behavioral data such as pre-swing, jump, vacate, and landing. Yunas and Ozanyan [13] extracted running fall features for screening based on conjugate smart sensors and used incremental learning algorithm for injury prevention.

With the advent of the big data era, traditional machine learning algorithms can no longer satisfy the researchers' pursuit of performance, and more and more scholars apply deep learning to the monitoring of track and field training behaviors. Ortiz-Echeverri et al. [14] firstly screened the features with neighborhood component analysis, and then classified the training behaviors by using a dense neural network, and the accuracy of the classification was only 72.17%. Zhang [15] used K-means algorithm to cluster non-positive training behaviors and BP neural network algorithm to monitor positive behaviors, but the accuracy was not high. Yang et al. [16] fixed a behavior monitoring device at the athlete's wrist to collect motor behavior data and used BP neural network to build a model for behavioral classification. Sung et al. [17] used a nine-axis posture angle sensor to collect training behavior data from track and field athletes and used RNN to classify training behaviors. Pan et al. [18] used data collected by a three-axis accelerometer to identify track and field training activities. The 3D raw accelerometer data can be directly used as input for training Convolutional Neural Network (CNN) models without any complex preprocessing. Na et al. [19] extracted the data from sensors, and then downscaled the data using Kernel-based Discriminant Analysis (KDA), and finally, applied it to training

behavior recognition by LSTM-based neural structured learning applied to training behavior recognition. Zhou et al. [20] designed a framework of Bi-LSTM for multimodal sensor fusion to sense and classify dangerous behaviors in daily training.

1.2. **Contribution.** It can be seen from the analysis of the above research status that the existing track and field training behavior monitoring methods have the problems of feature redundancy and low accuracy. To deal with the above issues, this article suggests a track and field training behavior monitoring method based on conjugate material intelligent sensors and neural networks. Firstly, the training behavior data of track and field athletes are collected using Conjugate Intelligent Sensors (CIS), and the behavior data are denoised using wavelet analysis. Secondly, the features hidden in the potential sensor signal variables are extracted using multivariate statistical analysis, and the features are downgraded using principal component analysis, so that the multidimensional features are recombined according to the corresponding ratios to highlight the effective dimensions. Finally, the attention mechanism is introduced into a one-dimensional CNN (1D-CNN) to enhance the key behavioral features in track and field training, the LSTM layer is used to learn the temporal features among the behavioral features cyclically, and the fully-connected layer is used to complete the behavioral classification and monitoring by applying weights.

2. Related theoretical analysis.

2.1. **Conjugate intelligent sensors.** CIS [21] refers to the incorporation of conjugate materials (usually organic or inorganic semiconductors) into intelligent sensors (acceleration sensors, gyroscope sensors, etc.), which have the advantages of being unaffected by light or temperature factors, being able to measure over long distances, having strong privacy protection, and being easy to install and arm. Conjugated material sensors can respond strongly to light or electrical signals with specific wavelengths because of their conjugated molecular structure, which makes them have significant advantages in detection sensitivity and selectivity.

The principle of CIS can be simply expressed as follows: when a molecule of a photoelectrochemically active substance is excited by a certain amount of light, it can be directly or indirectly transferred to the conduction band of the electrode of the semiconductor material by the electron regulation mechanism, thus generating a photocurrent. This light-driven principle has been widely used in the field of athletes' training behavior monitoring [22]. Figure 1 shows the schematic diagram of the conjugate semiconductor in CIS. The advantage of CIS in sports monitoring is that they can provide high sensitivity and selective monitoring, so as to accurately capture the subtle movement changes of athletes.

2.2. **Convolutional neural network.** CNN is a deep neural network structure, which has better performance and lower risk of overfitting than traditional neural networks [23]. The basic structure of CNN is indicated in Figure 2.

(1) **Convolutional level.** The convolution kernel, also known as a filter, transforms the matrix of the previous network into the unit matrix of the next network according to the size of the filter. The value of the i-th node in the unit matrix is as bellow.

$$g(i) = f\left(\sum_{x=x_1}^{n_1}\sum_{y=y_1}^{n_2}\sum_{z=1}^{n_3} a_{x,y,z}\cdot v_{x,y,z}^{j} + b^{i}\right) \tag{1}$$

where $a_{x,y,z}$ denotes the value of node (x, y, z) in the filter, $v_{x,y,z}^{j}$ denotes the weight of input node (x, y, z) of the filter, b^{i} denotes the bias term parameter of the output node,

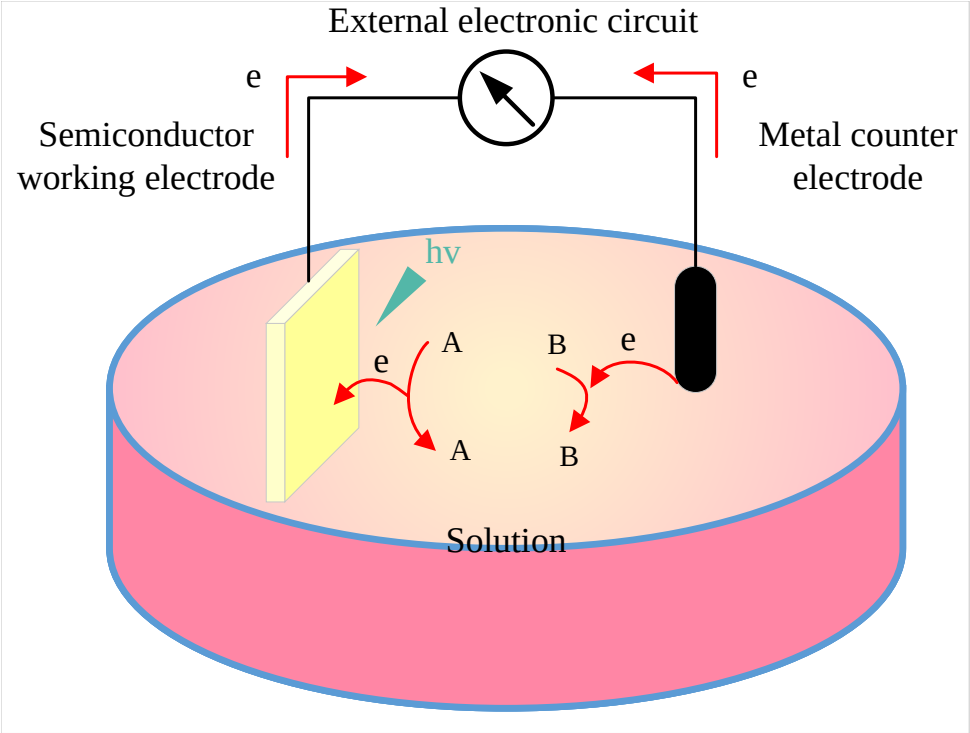

Figure 1. The schematic diagram of the conjugated semiconductor in CIS

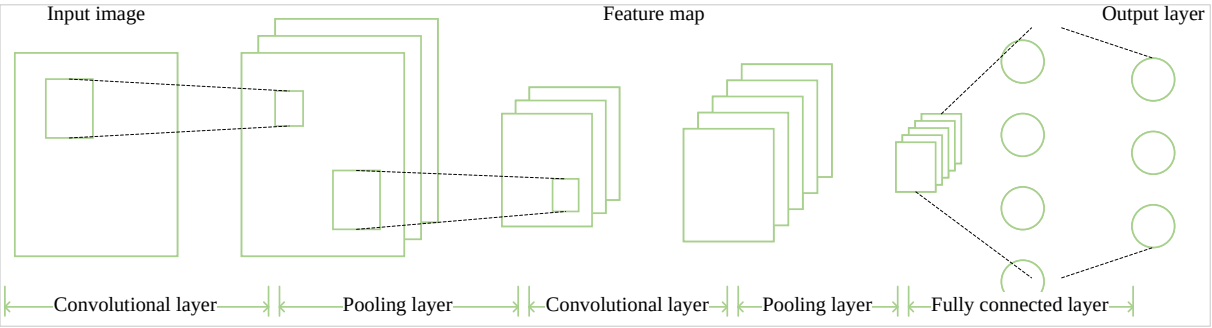

Figure 2. The basic structure of CNN

and f denotes the activation function. (2) **Pooling level.** The operation of pooling layer mainly consists of two strategies: average pooling and max pooling [24]. Average pooling is to find out the average response value of all feature channels from the normalized output:

$$R^i(x,y,z,i) = \frac{\sum_{x,y,z\in(x,y,z,i)} Q'(x,y,z,i)}{\left|N(x,y,z,i)\right|}. \tag{2}$$

Large pooling is taking the maximum response value for each feature channel from the normalized output:

$$R^i(\bar{x},\bar{y},\bar{z},i) = \max_{x,y,z\in(x,y,z,i)} Q'(x,y,z,i), \tag{3}$$

where $R^i(\bar{x},\bar{y},\bar{z},i)$ is the result of pooling the convolutional level, and $(\bar{x},\bar{y},\bar{z})$ represents the average value of position (x,y,z) within the pooled level $N(x,y,z,i)$.

(3) **Fully connected level.** The local features extracted from the convolutional level and pooling level are stitched together to form a complete image feature. Generally, there will be one or two fully connected levels to give the final classification result.

3. **Conjugate material-based smart sensors for track and field training behavioral data acquisition and denoising.** Prior to active monitoring of track and field training behaviors, athlete metrics need to be captured via a CIS. The CIS is placed on the athlete's body and a node is placed on the sensor to collect identifiable data. The number of conjugate semiconductors in the CIS is set to n, and the raw data collected by the i-th conjugate semiconductor is $x_i'(t)$. The collected data is normalized to obtain the collected track and field training behavior metrics as following:

$$x_i(t) = \frac{x_i'(t) - x_{i,\min}'(t)}{x_{i,\max}'(t) - x_{i,\min}'(t)}. \tag{4}$$

The actual coverage of the CIS sensor is then specified as bellow.

$$W = (1 + B - \sum_{U=1}^{N} o\,U + \lambda)^2 + F\,U, \tag{5}$$

where W denotes the actual coverage of the CIS sensor, N is a constant indicating the upper limit of the summation, o denotes the conversion ratio, U denotes the controllable sensing distance, λ denotes the repetitive sensing area, and F denotes the descriptive range.

After defining the coverage area, it is necessary to calculate the maximum permissible sensing difference of the CIS sensor, as indicated in the following:

$$E = \phi\, 2^*\, \xi(1 + l), \tag{6}$$

where E denotes the maximum sensing difference, ϕ denotes the recognizable range, ξ denotes the number of active recognitions, and l denotes the average value of controllable recognitions.

Secondly, a monitoring program is added to each conjugate semiconductor and linked to the initially deployed nodes, and the behavioral metrics are collected as indicated as follow:

$$X(t) = w_1 x_1(t) + w_2 x_2(t) + \cdots + w_i x_i(t) + \cdots + w_n x_n(t). \tag{7}$$

where $W < \varepsilon'$, $E < \varepsilon'$, and w_i denote the fusion weights of conjugate semiconductors in multiple CISs; ε denotes the coverage threshold; and ε' denotes the sensing error threshold.

As the CIS sensor will be affected by various disturbing factors when collecting data, such as the surrounding environment, psychological factors, physiological factors, etc., these disturbing factors will generate a lot of noise data, and if not filtered, the noise data will have a negative impact on the accuracy of subsequent monitoring. In this paper, wavelet analysis [25] is used for filtering and denoising, and the specific steps are as follow:

Step 1: Assumption $Y = X + m$, where Y is the band interference estimate of the message X and m is the component of noise.

Step 2: To get the noiseless variable X, we need to minimize the risk function and its value, which is calculated as follow:

$$R = \mathbb{E}\Big[\, C\Big(X, \tilde{X}\Big)\Big] = \int_{-\infty}^{\infty}\int_{-\infty}^{\infty} C\Big(X, \tilde{X}\Big)\, P_{X,Y}(x, y)\, dx\, dy, \tag{8}$$

where $\tilde{X}$ is the approximation of X and $P_{X,Y}$ is the density function corresponding to the random variable, the solution equation is implied in the next equation, and the chosen expression for the approximation error is $X_A = X - \tilde{X}$.

$$P_{X,Y}(x, y) = P(y)\, P_{X|Y}(x \,|\, y) \tag{9}$$

Step 3: Derive the expression for the prior distribution risk function R as follows:

$$R = \int_{-\infty}^{\infty} P_Y(y) \left[\int_{-\infty}^{\infty} C\left(X, \tilde{X}\right) P_{X|Y}(x \mid y)\, dx \right] dy. \tag{10}$$

The first part of the above equation is a constant, and to minimize the risk factor R, it is necessary to ensure that the second half is minimized. The Bayes approximation is obtained by derivation:

$$-2\left[\int_{-\infty}^{\infty} x\, P_{X|Y}(x \mid y)\, dx\right] + 2\,\tilde{X}\left[\int_{-\infty}^{\infty} P_{X|Y}(x \mid y)\, dx\right] = 0. \tag{11}$$

When $2\,\tilde{X}\int_{-\infty}^{\infty} P_{X|Y}(x \mid y)\, dx = 1$, the corresponding observed signal approximation is $\tilde{X}_{ms}$ and the corresponding Bayesian function are indicated below, respectively:

$$\tilde{X}_{ms} = \int_{-\infty}^{\infty} x\, P_{X|Y}(x \mid y)\, dx \tag{12}$$

$$R = \int_{-\infty}^{\infty} \left(P_{Y|y}\right) \left[1 - \int_{-\tilde{X}+\frac{\tau}{2}}^{\tilde{X}-\frac{\tau}{2}} P_{X|Y}(x \mid Y)\, dx\right] dy. \tag{13}$$

After the above calculation, the threshold formed by the automatic segmentation can be derived to carry out the wavelet reconstruction of the signal, i.e., the filtered signal is wavelet inverted, and the denoised behavioral data $X'(t)$ is obtained.

4. Track and field training behavior monitoring based on conjugate material smart sensor and neural network.

4.1. Feature extraction and dimensionality reduction of track and field training behavioral data based on CIS sensors.

To accurately monitor the track and field training behaviors, this paper first extracts the features of the collected signal data using multivariate statistical Factor Analysis (FA) [26], then uses Principal Component Analysis (PCA) [27] to and the entire model is indicated in Figure 3.

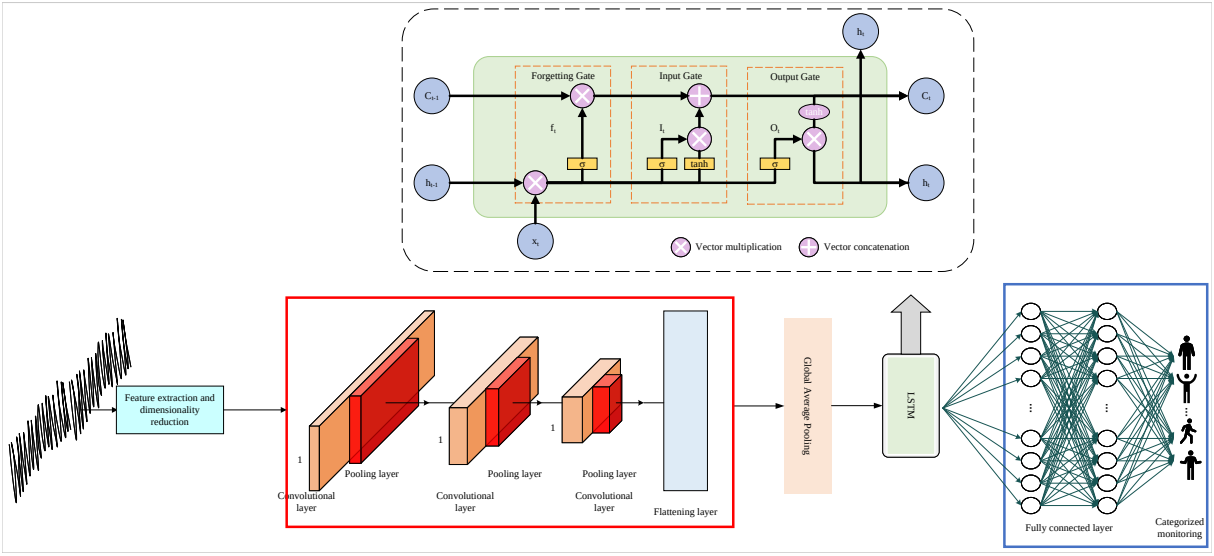

Figure 3. The entire model of the suggested behavioral monitoring methods

The CIS sensor acquisition data after wavelet noise reduction filters out most of the noise, but still contains behavioral signals with different characteristics. FA interprets the observed variables as linear combinations of several potential factors with specific factors,

and searches for the characteristics hidden in these potential variables by investigating the internal relationship between multiple signal variables.

$$X' = LF + E \tag{14}$$

where X denotes the vector of observed variables, F denotes the vector of latent variables, E denotes the vector of sensing errors of the CIS, and L is the matrix of eigenvectors, which represents the linear relationship between the observed variables and the latent variables.

$$\mathcal{L}(L) = -\frac{1}{2}\ln|\psi| - \frac{1}{2}\operatorname{Tr}\left(\psi^{-1}S\right) + \frac{1}{2}\operatorname{Tr}\left(\psi^{-1}LSL^{\top}\right) \tag{15}$$

where S is the covariance matrix of the observed variables and ψ is the covariance matrix of the error term.

To accurately monitor the training behavior of track and field, it is necessary to carry out feature dimensionality reduction of the extracted features, because high-dimensional features will reduce the efficiency of monitoring, and the phenomenon of "over-training" will also occur. Therefore, principal component analysis is used to reduce the dimensionality of the extracted features and remove the redundancy of the features. The steps are as bellow.

Step 1: Centering all data samples. Generate a matrix X using the original data, and then calculate the new matrix X obtained by subtracting the mean value of each dimension of data in X from that dimension.

$$x_i = x_i - \frac{1}{m}\sum_{j=1}^{m} x_j \tag{16}$$

where x_i represents the samples in matrix X, m represents the number of samples in matrix X, and j represents a random number, with j taking the range $(0, m]$. Calculate the covariance matrix C using Equation (17).

$$C = \frac{1}{m}XX^T \tag{17}$$

Step 2: Sort the eigenvalues of L in descending order, and take the eigenvectors corresponding to the first k eigenvalues to form a matrix U. The value of k can be obtained from $\left((\sum_{i=1}^{k}\mu_i)/(\sum_{i=1}^{n}\mu_i)\right) \geq t$, where n represents the number of eigenvalues, k represents the number of eigenvalues taken, and the range of values is $[1, n]$, μ_i is the i-th eigenvalue, and s is the weighting threshold for the main component, and the range of values is $(0, 1]$.

Step 3: Construct the principal component matrix based on the number p of principal components of the feature matrix.

$$Z_{m\times p} = X_{m\times p}\, U_{m\times q} \tag{18}$$

where $U_{m\times p} = [L_1, L_2, \ldots, L_p]$, and finally the principal component feature $Z_{m\times p}$ after PCA feature dimensionality reduction is obtained.

4.2. **Convolutional neural network-based behavior monitoring for track and field training.** To better capture the temporal order and relevance of track and field training behavior data, this paper firstly introduces the channel attention mechanism in 1D-CNN, which generates a weight matrix from 0 to 1 based on the input feature map, and then uses it to weight the feature map to indicate the degree of relevance of a certain part of behavioral features to the key information. The channel attention mechanism focuses on the interdependence of the channel feature matrices in the input feature map, and automatically learns the importance of each feature channel through a multilayer

perceptron, and weights each channel feature with it. The generation of channel attention map in 1D-CNN is indicated in Equation (19).

$$M_c(Z) = \delta\big(\mathrm{MLP}(\mathrm{AvgPool}(Z)) + \mathrm{MLP}(\mathrm{MaxPool}(Z))\big) = \delta\big(V_1\big(V_0(Z^c_{\mathrm{avg}})\big) + V_1\big(V_0(Z^c_{\mathrm{max}})\big)\big) \tag{19}$$

where the number of neurons in the obscured level of the MLP is C/r; C is the amount of channels in the feature map; r is the compression ratio; δ is the sigmoid function; V_0 and V_1 are the network weights of the multilayer perceptual machine; Z^c_{avg} and Z^c_{max} are the channel dimensional feature maps obtained after maximal pooling and average pooling, respectively.

Spatial attention focuses on the positional relationships between features in the feature map and uses a convolutional layer to learn the importance of each part of the features. The spatial attention map is generated as implied in Equation (20).

$$M_s(Z) = \delta\big(f^k\big([\mathrm{AvgPool}(Z); \mathrm{MaxPool}(Z)]\big)\big) = \delta\big(f^k\big([Z^s_{\mathrm{avg}}; Z^s_{\mathrm{max}}]\big)\big) \tag{20}$$

where f^k is a one-dimensional convolution with kernel size k.

The sigmoid function is then used to generate the weight information for each channel $G = [g_1, g_2, \ldots, g_c]$. The obtained weight values are used to scale the feature map to obtain the CBAM-enhanced key features $\tilde{Z}$.

$$\tilde{Z} = [\tilde{z}_1, \tilde{z}_2, \ldots, \tilde{z}_c] \ (\tilde{Z} \in \mathbb{R}^{l\times 1\times C}) \tag{21}$$

where $\tilde{z}_C = L_c \cdot g_c$.

After obtaining the above key features, this article slices the feature map into sequences according to time, which are sequentially input into the LSTM layer for training to learn the temporal order of the features. The forgetting stage uses the forgetting gate to weight the internal state to realize the forgetting of long-term memory; the remembering stage uses the input gate to save the important features into the internal state to complete the updating of long-term memory. The output stage uses the output gate to select the output information from the internal state. The formula for the internal processing is as follows.

$$f_t = \delta(V_{xf} \cdot x_t + V_{hf} \cdot h_{t-1} + b_f) \tag{22}$$

$$i_t = \delta(V_{xi} \cdot \tilde{z}_t + V_{hi} \cdot h_{t-1} + b_i) \tag{23}$$

$$\tilde{C}_t = \tanh(V_{xc} \cdot \tilde{z}_t + V_{hc} \cdot h_{t-1} + b_c) \tag{24}$$

$$C_t = f_t \odot C_{t-1} + i_t \odot \tilde{C}_t \tag{25}$$

$$o_t = \delta(V_{xo} \cdot \tilde{z}_t + V_{ho} \cdot h_{t-1} + b_o) \tag{26}$$

where f_t, i_t, and o_t represent the forgetting, input, and output gates of the LSTM cell, respectively, which control the discarding, memorizing, and outputting of the information in the cell; C_t is the temporal information of the key features; V denotes the weights; and b denotes the bias.

With the interaction of the three gate structures mentioned above, the final output value of the LSTM monolithic structure is obtained, which can be expressed as Equation (27).

$$h_t = o_t \odot \tanh(C_t) \tag{27}$$

The obscured state output from the last step is fed into two consecutive fully connected layers to monitor the classification of track and field training behaviors. After the fully connected layer, a dropout level [28] is added to prevent network overfitting with a certain

probability and improve the generalization ability. Finally, the monitoring results are output by Softmax function.

$$\text{Softmax}(h_t) = \frac{\exp(h_t)}{\sum_{r=1}^{N} \exp(h_r)} \tag{28}$$

5. Performance testing and analysis.

5.1. Performance analysis of behavioral monitoring for athletic training.

In this article, the validity of the suggested method is verified by using the training behavior dataset of track and field athletes collected from the literature [29], which contains five types of behaviors of pre-swinging, jumping, vacating, landing, and assisting running in track and field training. The dataset is divided into training set (1039 samples) and test set (237 samples) according to the ratio of 7:3 and the method PSWSDS in the literature [16], the method CNNABR in the literature [18], the method SSCNLT in the literature [19], and the method CSICNN are evaluated in this paper, and the learning rate during the training is set to 0.01, and the optimizer uses Adam. The experimental environment is Centos7 operating system, the CPU is Intel Xeon 4210R@2.40Ghz, the GPU is NVIDIA RTX 2080Ti, the programming language is Python 3.6, and the training framework used is Tensorflow 2.3.

This article uses the statistical metrics commonly used in the performance evaluation of classification problems: Mean Accuracy, Composite Accuracy (sAcc), Precision (Prec), Recall (Rec), and F1 Score as the evaluation metrics for monitoring performance.

A comparison of the accuracy rates of monitoring track and field training behaviors using four different monitoring methods is indicated in Table 1. The average monitoring accuracy of the CSICNN method was 90.5%, which was higher than that of the PSWSDS, the CNNABR and the SSCNLT, and it was the most effective. The monitoring accuracy of vacating behaviors was higher than that of other movements, and the accuracy rates of both the CSICNN and the SSCNLT were 85% or higher than that of other movements. The accuracy of CSICNN and SSCNLT were both above 85%, but the accuracy of CSICNN's pre-swing and run-assist was lower than that of the other behaviors because of the similarity of pre-swing and run-assist in the longitudinal movement, which could lead to incorrect monitoring. PSWSDS utilized the BP neural network to monitor the behaviors, but it was hard to address the multiclassification issue, and the effect of the monitoring was poor. CNNABR, although it utilized the CNN to monitor the behaviors, but it did not remove the redundant features. features, so the accuracy of track and field training behavior is worse than CSICNN and SSCNLT.

Table 1. Comparison of the accuracy results of the four methods

Action	PSWSDS	CNNABR	SSCNLT	CSICNN
pre-sweep	0.731	0.781	0.849	0.881
jump	0.757	0.762	0.828	0.902
vacate	0.784	0.824	0.856	0.935
land	0.738	0.811	0.796	0.912
run	0.766	0.795	0.817	0.896

Figure 4 shows the comparison of the performance results of different track and field training behavior monitoring methods. As can be seen from the figure, the CSICNN method has 89.5% sAcc, 91.1% Prec, 89.3% Rec, and 90.2% F1-Score. The accuracy

of the CSICNN method is at least 5.8% higher than the other three methods, and the Prec, Rec, and F1-score are also the highest among these methods. The monitoring performance of the SSCNLT is closest to that of the RCSICNN due to the fact that although it utilizes the KDA for dimensionality reduction on the collected sensor data, it does not extract the important features of the internal data. The CNNABR's monitoring performance is second only to SSCNLT, with 79.9% sAcc, 78.1% Prec, 76.2% Rec, and 77.1% F1-Score, and it does not perform feature dimensionality reduction on the collected behavioral data and does not take into account the temporal nature of the features, and thus the monitoring performance is much worse than that of the CSICNN. The PSWSDS performs the worst, and it directly uses the collected behavioral data as the input to the BP neural network, did not process the behavioral data for noise reduction, and did not consider the temporal nature of the track and field training behavioral data. The experiment demonstrated that CSICNN obtained the best monitoring effect among the four methods.

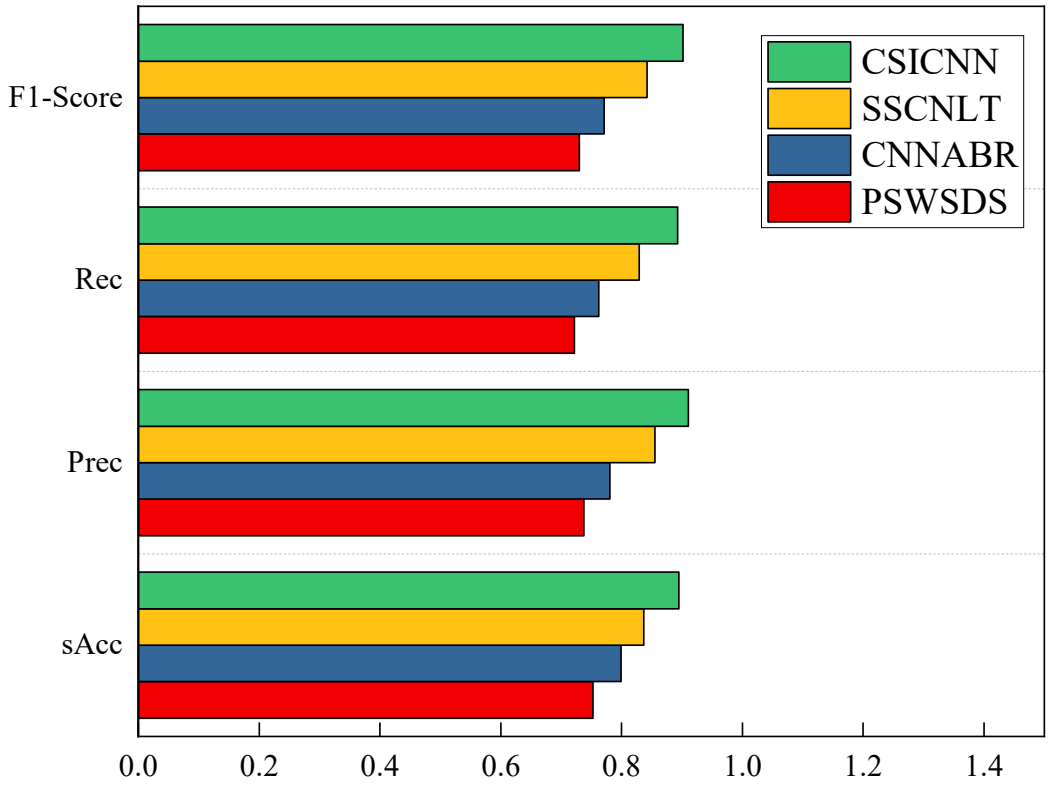

Figure 4. Comparison of monitoring performance of four methods

5.2. Comparison of time consumed and lost for behavioral monitoring of track and field training. Table 2 compares the monitoring consumption time of CSICNN with other methods. The training time, testing time and classification time of CSICNN are 297.18 s, 0.47 s and 3.59 s respectively, which are the lowest in terms of training time (300 cycles), testing time and classification time relative to the other three methods. This indicates that the CSICNN algorithm takes less time to train, and when the sample size increases, the training time of the model increases, and fast training saves more time. SSCNLT has the next lowest time consumption for each of the time consumptions, which is due to the fact that it does not perform noise reduction on the behavioral data, which results in a higher time consumption than that of the CSICNN. The training time, testing

time, and classification time are longer for both PSWSDS and CNNABR because they do not apply noise reduction to the behavioral data.

Table 2. TABLE 2. Comparison of consumption time for different monitoring methods

Method	Training time (s)	Test time (s)	Sorting time (s)
PSWSDS	9173.82	13.18	85.19
CNNABR	3595.08	8.09	39.47
SSCNLT	817.69	1.26	12.07
CSICNN	297.18	0.47	3.59

The loss curves for the four monitoring methods are indicated in Figure 5. The loss value decreases rapidly in the first 20 iterations, and the computational burden increases as the number of iterations increases. Then, the loss value of CSICNN slowly oscillates downward and tends to converge, and finally the loss value stabilizes at about 1. The loss values of PSWSDS, CNNABR, and SSCNLT are relatively close to each other, but the difference is that the loss of SSCNLT is obviously lower than that of PSWSDS and CNNABR in the first 20 iterations. The CSICNN has the lowest loss and better stability.

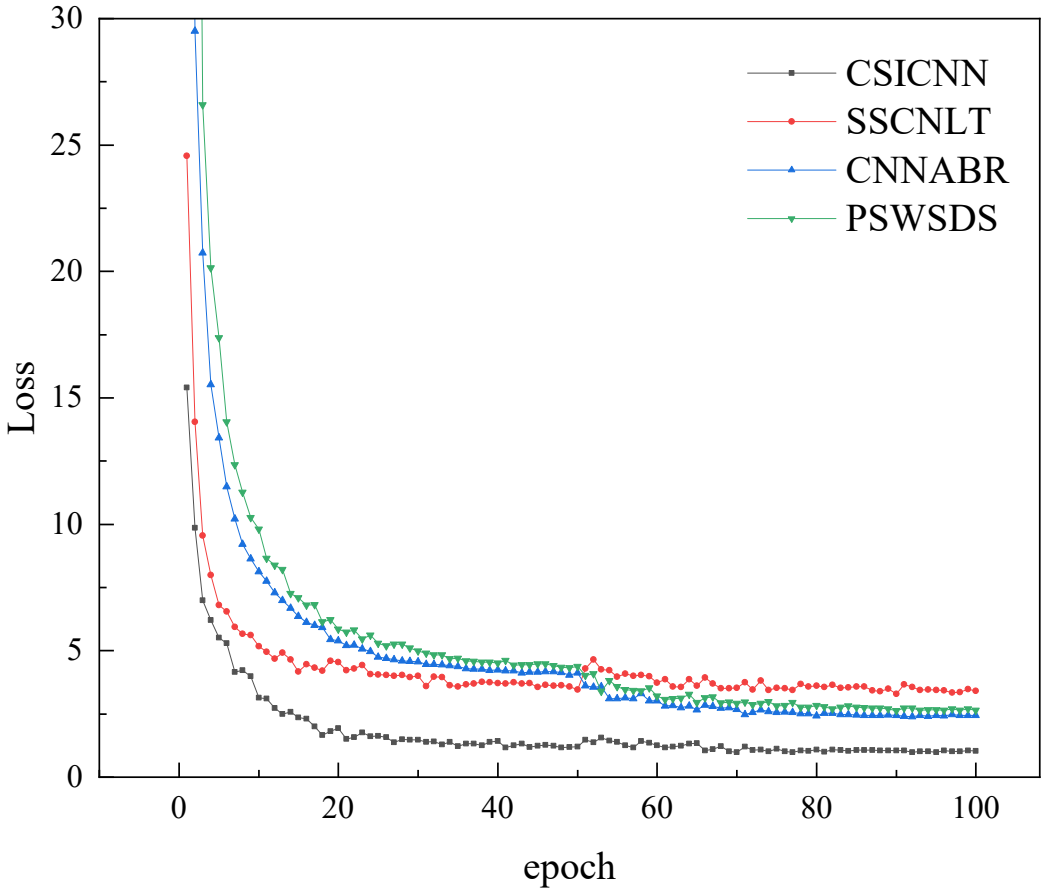

Figure 5. Comparison of losses from different monitoring methods

6. **Conclusion.** Intending to the issue that existing track and field training behavior monitoring methods ignore the key features of behavior and have low accuracy, this article suggests a track and field training behavior monitoring method based on conjugate

material intelligent sensors and neural networks. Firstly, the training behavior data of track and field athletes are collected using conjugate material intelligent sensors, and the collected behavior data are denoised using wavelet analysis. Secondly, the features of the behavioral data are extracted using multivariate statistical analysis, and the features are downscaled using principal component analysis, so that the multidimensional features are recombined together according to the corresponding ratio to reduce the interference factor. Finally, the attention mechanism is introduced into 1D-CNN to enhance the key behavioral features in track and field training, and the LSTM layer is used to learn the temporal features among the behavioral features in a cyclic manner, and the fully-connected layer is used to complete the behavioral classification and monitoring by applying weights. The experimental outcome implies that the designed method has higher monitoring performance and efficiency compared with the other three methods.

Acknowledgment. This work is supported by the Anhui Provincial Universities Scientific Research Project (No. 2024AH052552).

REFERENCES

[1] B. H. DeWeese, G. Hornsby, M. Stone, and M. H. Stone, "The training process: Planning for strength–power training in track and field. Part 1: Theoretical aspects," *Journal of Sport and Health Science*, vol. 4, no. 4, pp. 308–317, 2015.

[2] D. J. Huxley, D. O'Connor, and P. A. Healey, "An examination of the training profiles and injuries in elite youth track and field athletes," *European Journal of Sport Science*, vol. 14, no. 2, pp. 185–192, 2014.

[3] T.-Y. Wu, H. Li, S. Kumari, and C.-M. Chen, "A Spectral Convolutional Neural Network Model Based on Adaptive Fick's Law for Hyperspectral Image Classification," *Computers, Materials & Continua*, vol. 79, no. 1, pp. 19–46, 2024.

[4] T.-Y. Wu, A. Shao, and J.-S. Pan, "CTOA: Toward a Chaotic-Based Tumbleweed Optimization Algorithm," *Mathematics*, vol. 11, no. 10, p. 2339, 2023.

[5] T.-Y. Wu, H. Li, and S.-C. Chu, "CPPE: An Improved Phasmatodea Population Evolution Algorithm with Chaotic Maps," *Mathematics*, vol. 11, no. 9, p. 1977, 2023.

[6] A. Chen, J. Zhang, L. Zhao, R. D. Rhoades, D.-Y. Kim, N. Wu, J. Liang, and J. Chae, "Machine-learning enabled wireless wearable sensors to study individuality of respiratory behaviors," *Biosensors and Bioelectronics*, vol. 173, 112799, 2021.

[7] Z. Xue, D. Ming, W. Song, B. Wan, and S. Jin, "Infrared gait recognition based on wavelet transform and support vector machine," *Pattern Recognition*, vol. 43, no. 8, pp. 2904–2910, 2010.

[8] S. Balli, E. A. Sağbaş, and M. Peker, "Human activity recognition from smart watch sensor data using a hybrid of principal component analysis and random forest algorithm," *Measurement and Control*, vol. 52, no. 1–2, pp. 37–45, 2019.

[9] W. A. Welch, D. R. Bassett, D. L. Thompson, P. S. Freedson, J. W. Staudenmayer, D. John, J. A. Steeves, S. A. Conger, T. Ceaser, and C. A. Howe, "Classification accuracy of the wrist-worn GENEA accelerometer," *Medicine and Science in Sports and Exercise*, vol. 45, no. 10, p. 598, 2013.

[10] K. Xia, H. Wang, M. Xu, Z. Li, S. He, and Y. Tang, "Racquet sports recognition using a hybrid clustering model learned from integrated wearable sensor," *Sensors*, vol. 20, no. 6, 1638, 2020.

[11] Y. H. Lee, M. Jang, M. Y. Lee, O. Y. Kweon, and J. H. Oh, "Flexible field-effect transistor-type sensors based on conjugated molecules," *Chem*, vol. 3, no. 5, pp. 724–763, 2017.

[12] J. Shanthini, P. Arunkumar, S. Karthik, and N. Karthikeyan, "Interpretation of Gait Supervising Mechanism Using Sensor Integrated Makeshift and Analysing Pattern by K-Means Clustering Algorithm," *Journal of Medical Imaging and Health Informatics*, vol. 11, no. 10, pp. 2598–2609, 2021.

[13] S. U. Yunas and K. B. Ozanyan, "Gait activity classification using multi-modality sensor fusion: a deep learning approach," *IEEE Sensors Journal*, vol. 21, no. 15, pp. 16870–16879, 2021.

[14] C. J. Ortiz-Echeverri, S. Salazar-Colores, J. Rodríguez-Reséndiz, and R. A. Gómez-Loenzo, "A new approach for motor imagery classification based on sorted blind source separation, continuous wavelet transform, and convolutional neural network," *Sensors*, vol. 19, no. 20, 4541, 2019.

[15] Y. Zhang, "Track and field training state analysis based on acceleration sensor and deep learning," *Evolutionary Intelligence*, vol. 16, no. 5, pp. 1627–1636, 2023.

[16] J. Yang, C. Meng, and L. Ling, "Prediction and simulation of wearable sensor devices for sports injury prevention based on BP neural network," *Measurement: Sensors*, vol. 33, 101104, 2024.
[17] J. Sung, S. Han, H. Park, H.-M. Cho, S. Hwang, J. W. Park, and I. Youn, "Prediction of lower extremity multi-joint angles during overground walking by using a single IMU with a low frequency based on an LSTM recurrent neural network," *Sensors*, vol. 22, no. 1, 53, 2021.
[18] Z. Pan, H. Chen, W. Zhong, A. Wang, and C. Zheng, "A CNN-based animal behavior recognition algorithm for wearable devices," *IEEE Sensors Journal*, vol. 23, no. 5, pp. 5156–5164, 2023.
[19] Y. Na, S. El-Tawil, A. Ibrahim, and A. Eltawil, "Stick-slip classification based on machine learning techniques for building damage assessment," *Journal of Earthquake Engineering*, vol. 26, no. 11, pp. 5848–5865, 2022.
[20] T. Zhou, A. Tao, L. Sun, B. Qu, Y. Wang, and H. Huang, "Behavior recognition based on the improved density clustering and context-guided Bi-LSTM model," *Multimedia Tools and Applications*, vol. 82, no. 29, pp. 45471–45488, 2023.
[21] R. Song, Z. Wang, X. Zhou, L. Huang, and L. Chi, "Gas-sensing performance and operation mechanism of organic π-conjugated materials," *ChemPlusChem*, vol. 84, no. 9, pp. 1222–1234, 2019.
[22] S.-Z. Chen, G. Wu, and T. Xing, "Deflection monitoring for a box girder based on a modified conjugate beam method," *Smart Materials and Structures*, vol. 26, no. 8, 085034, 2017.
[23] Z. Li, F. Liu, W. Yang, S. Peng, and J. Zhou, "A survey of convolutional neural networks: analysis, applications, and prospects," *IEEE Transactions on Neural Networks and Learning Systems*, vol. 33, no. 12, pp. 6999–7019, 2021.
[24] M. Sun, Z. Song, X. Jiang, J. Pan, and Y. Pang, "Learning pooling for convolutional neural network," *Neurocomputing*, vol. 224, pp. 96–104, 2017.
[25] A. Halidou, Y. Mohamadou, A. A. A. Ari, and E. J. G. Zacko, "Review of wavelet denoising algorithms," *Multimedia Tools and Applications*, vol. 82, no. 27, pp. 41539–41569, 2023.
[26] H.-W. Cho, "Nonlinear feature extraction and classification of multivariate data in kernel feature space," *Expert Systems with Applications*, vol. 32, no. 2, pp. 534–542, 2007.
[27] H. Abdi and L. J. Williams, "Principal component analysis," *Wiley Interdisciplinary Reviews: Computational Statistics*, vol. 2, no. 4, pp. 433–459, 2010.
[28] A. Poernomo and D.-K. Kang, "Biased dropout and crossmap dropout: learning towards effective dropout regularization in convolutional neural network," *Neural Networks*, vol. 104, pp. 60–67, 2018.
[29] Y. Zhang, "Track and field training state analysis based on acceleration sensor and deep learning," *Evolutionary Intelligence*, vol. 16, no. 5, pp. 1627–1636, 2023.